Available online at www.sciencedirect.com
ScienceDirect

Global and Planetary Change 60 (2008) 471–486

GLOBAL AND PLANETARY CHANGE

www.elsevier.com/locate/gloplacha

Ecological and morphological response of brackish tidal marshland to the next century of sea level rise: Westham Island, British Columbia

Matthew L. Kirwan *, A. Brad Murray

Nicholas School of the Environment and Earth Sciences, Center for Nonlinear and Complex Systems, Duke University, Box 90227, Durham NC 27708 USA

Received 17 January 2007; received in revised form 2 May 2007; accepted 11 May 2007
Available online 22 June 2007

Abstract

In response to climatic warming, eustatic sea level has been predicted to rise by about 50 cm in the next century. While feedbacks between vegetation growth and sediment deposition tend to allow marshes to maintain their morphology under a constant rate of sea level rise, recent observations of marsh deterioration suggest that changes in the rate of sea level rise may induce loss of economically and ecologically important marshland. We have developed a three dimensional model of tidal marsh evolution that couples vegetation growth and sediment transport processes including bed accretion and wave erosion. We use the model to simulate the response of marshes and tidal flats along the Fraser River Delta, British Columbia to 100 yr forecasts of sea level change. Under low sea level-rise scenarios, the delta and its marshes prograde slightly, consistent with historical measurements. While accretionary processes greatly mediate the response to increased rates of sea level rise, vegetation zones transgress landward under median and high sea level rise rate scenarios. In these scenarios, low marsh erosion and constriction of high marsh vegetation against a dyke at its landward edge result in a 15–35% loss of marshland in the next century. Several important behavioral changes take place after 2050, suggesting that predictions based on field observations and short term model experiments may not adequately characterize (and sometimes underestimate) long-term change. In particular, the replacement of highly productive high marsh vegetation by less productive low marsh vegetation results in continued reduction of the system's total biomass productivity, even as the rate of loss of vegetated area begins to decline.

Keywords: sea level; accretion; erosion; ecogeomorphology; wave; wetland

1. Introduction

Tidal marshes are among the world's most ecologically productive and economically valuable ecosystems, but have recently been degrading to unvegetated mudflats or open water in many regions (Costanza et al., 1997). Tidal marshes provide habitat and nursery grounds for commercially important fin and shellfish, buffer coastal cities from storms, trap contaminants, and supply abundant organic matter to estuarine and marine environments (e.g. Turner, 1977; Patrick, 1994; Costanza et al., 1997; Mitsch and Gosselink, 2000). High sea level rise rates and low sediment supply rates are at least partially responsible for their recent decline. For

* Corresponding author.
E-mail addresses: mlk13@duke.edu (M.L. Kirwan), abmurray@duke.edu (A.B. Murray).

0921-8181/$ - see front matter © 2007 Elsevier B.V. All rights reserved.
doi:10.1016/j.gloplacha.2007.05.005

example, vertical accretion rates that are slower than relative sea level rise rates have resulted in submergence of wetlands in Louisiana and the Chesapeake Bay region, where sediment has been diverted and rates of subsidence are high (e.g. Reed, 1995; Kearney et al., 2002). In other regions, marsh loss is dominated by erosion from waves or channels rather than vertical submergence. In New York and southeast England, the edges of marshes have been retreating in response to increased wave erosion while the interior marshland has been eroding due to channel widening and lengthening (Hartig et al., 2002; Van der Wal and Pye, 2004).

Despite losses of marshland in certain regions, long-term vertical accretion rates typically mimic sea level rise rates, suggesting that tidal marshes are generally in long-term equilibrium with sea level (Friedrichs and Perry, 2001). An increase in the rate of sea level rise typically leads to increased inundation and sediment delivery to the marsh platform, increasing its rate of accretion. An increase in water depth on the platform may also stimulate the growth of vegetation which traps sediment, further enhancing deposition rates (Morris et al., 2002). These positive relationships between inundation and accretion tend to stabilize the response of marshes to changes in rates of sea level rise, allowing a marsh to maintain its general morphology and biological productivity (Morris et al., 2002; Kirwan and Murray, 2005, 2007). However, more frequent and deeper inundation will tend to increase the volume of water flowing through the channel network and may cause the network to expand at the expense of the vegetated marsh platform (Allen, 1997). In marshes subject to wave erosion, greater tidal flat depths may decrease dissipation of wave energy and lead to greater erosion rates near the marsh margin.

A number of one-dimensional numerical models of marsh accretion have been used to explore how a marsh platform will respond to sea level change (e.g. French, 1993; Allen, 1995; Morris et al., 2002). In these models, the marsh platform accretes at a rate proportional to its depth below high tide, a proxy for inundation frequency and duration. These models predict that under a constant rate of sea level rise, a marsh deep in the tidal frame will accrete at rates greater than the rate of sea level rise. Accretion rates decline as the platform gains elevation relative to sea level, until the platform reaches an equilibrium water depth where accretion equals sea level rise. An increase in the rate of sea level rise or a decrease in the rate of sediment delivery will temporarily cause accretion rates to fall behind sea level rise rates, and the platform will deepen. Deepening continues until deposition rates (increasing with depth) match the sea level rise rate and the platform reaches a new equilibrium.

Several complications challenge the ability of existing models to predict how intertidal surfaces respond to environmental change such as changes in rates of sea level rise or sediment delivery. Suspended sediment concentrations, for example, decrease with distance from the nearest channel and strongly influence patterns and rates of platform accretion (Friedrichs and Perry, 2001). This suggests that one-dimensional accretion models cannot fully address marsh morphodynamics. Models with spatially variable accretion rates (e.g. Reyes et al., 2000; Mudd et al., 2004) do capture these effects, but do not allow for changes in the channel network, which could alter the amount of sediment available for accretion. Recent models have started to address the coupled evolution of marsh platforms and channel networks, but these are neither intended nor suited for the prediction of a specific marsh's response to sea level rise (Kirwan and Murray, 2007; D'Alpaos et al., 2007). Following Morris et al. (2002), these models assume that vegetation productivity increases with depth, as observed in a South Carolina *Spartina alterniflora* salt marsh. In other regions, however, increasing inundation appears to decrease productivity (e.g. Reed and Cahoon, 1992). In such cases, accelerated sea level rise may lead to less productive vegetation, which would lead to slower accretion and facilitate more rapid submergence. This response differs fundamentally from the stability predicted by models that involve increasing biomass productivity and accretion. Finally, wave erosion determines the seaward extent of tidal marshland in many locations (e.g. Van der Wal and Pye, 2004). Existing models relate wave erosion to bed elevation and vegetation density, but do not consider sea level rise (van de Koppel et al., 2005). If accelerated sea level rise causes a deepening of intertidal surfaces, as other models suggest (French, 1993; Morris et al., 2002; Kirwan and Murray, 2007), then the rate of wave erosion would be expected to increase with the rate of sea level rise.

Atmosphere–Ocean General Circulation Models (AOGCMs) project an acceleration of global sea level during the current century (IPCC, 2001). Although considerable uncertainty exists, a median scenario of sea level rise involves a global rate change from the late Holocene average of about 1 mm/yr to rates of about 6 mm/yr by 2100, and a total rise of about 40 cm. Higher scenarios involve maximum rates of about 11 mm/yr. Estimating a critical sea level rise rate that would drown marshes remains problematic, and depends on the local sediment supply and properties of vegetation. For example, marshes on the Yangtze River Delta accrete 14–25 mm/yr (e.g. Yang et al., 2003), while widespread deterioration of marshes has already occurred in the sediment starved Chesapeake Bay and Louisiana regions, where rates of relative sea level rise are about 3 mm/yr and 10 mm/yr, respectively (Reed, 1995; Kearney et al., 2002). Numerical models demonstrate that when vegetation is intact, marsh platforms maintain an intertidal position under wide ranges of sediment delivery and sea level rise rates exceeding 10 mm/yr (Morris et al., 2002; Kirwan and Murray, 2007). However, disturbance to vegetation can cause the platform to be unstable and prone to drowning, at much lower rates (Kirwan and Murray, 2007).

In some marshes responding to sea level rise, intertidal vegetation migrates landward by replacing forestland (e.g. Brinson et al., 1985; Williams et al., 1999; Kirwan et al., 2007). In other areas, steep slopes or artificial dykes prevent landward migration of vegetation, meaning that any loss of marsh at the seaward side cannot be compensated by landward expansion (e.g. Van der Wal and Pye, 2004). However, the presence of a dyke does not guarantee a reduction of marsh area. Marshes bounded by a dyke may build vertically in equilibrium with the rate of sea level rise, or even expand in the seaward direction (e.g. Van der Wal and Pye, 2004). This variability in marsh behavior, including observed deterioration in several regions worldwide, raises several important questions about how tidal surfaces will respond to future sea level change:

1) How will accretion rates and intertidal water depths respond to forecasted sea level scenarios?
2) How will vegetation productivity and zonation patterns respond to sea level change?
3) Where and when are changes to substrate and vegetation most evident?

Given the economic and ecological importance of tidal marshes, it is important to fully understand their response to sea level rise. Developing fully coupled models of marsh accretion, erosion, and vegetation, is an important step towards management of this ecosystem. We address the questions above by simulating the response of marshes to various sea level projections with a coupled model of vegetation productivity, vertical accretion, and wave erosion. We focus on the marshes and tidal flats along a portion of the Fraser River Delta, British Columbia, as a case study. A dyke bounds the landward edge of this marsh, meaning that we can ignore the complex interactions between marsh and terrestrial vegetation that would govern the expansion of marshland in the landward direction. We use a highly simplified numerical model that only incorporates processes hypothesized to be most essential in governing long-term behavior. For example, in this particular area, we assume marshland erodes primarily due to waves rather than channel currents (Hill, 2006). Consequently, the computationally intensive hydrodynamic flow routing included in other models of marsh morphology (Kirwan and Murray, 2007; D'Alpaos et al., 2007) is not needed. These simplifications allow the model to simulate a large area (5 km^2) over the next century. However, since a number of more detailed processes (e.g. distinguishing between above-ground sediment trapping and below-ground organic matter accumulation in estimates of substrate accretion) are not incorporated, the results of the modeling should be viewed as an initial exploration of basic behavior rather than a precise simulation. In this contribution, we focus on how different sea level and subsidence scenarios may affect the biological productivity and morphologic stability of intertidal surfaces. We are not aware of any other simulations that model the response of marsh morphology and ecology to IPCC sea level projections.

2. Study area

The Fraser River delta is an accumulation of Holocene sediment where the Fraser River meets the Georgia Strait, in southwestern British Columbia, Canada (Fig. 1). The delta has accumulated since about 9000 BP (C-14 yr), prograding seaward at an average rate of 2.4 m/yr since 2250 BP (Williams and Roberts, 1989). Relative sea level inferred from Fraser River Delta sediments (Williams and Roberts, 1989), and elsewhere in the region (e.g. Long and Shennan, 1998), rose about 1 mm/yr over similar time scales. Westham Island, part of the Fraser River delta, is bounded by the Main Arm of the Fraser River and Canoe Pass. Mean tidal range is about 3.5 m (Canadian Hydrographic Service, 2006). From seaward to landward, intertidal surfaces typically consist of sandflats, mudflats, and marshland. Marshland consists of brackish water species including, from seaward to landward, *Scirpus americanus*, *Carex lyngbyei*, *S. maritimus*, and *Typha* sp. Shaw et al. (2006) consider the distribution of vegetation zones in more detail. A dyke separates the intertidal flats and marshland from agricultural lands along the entire length of Westham Island.

The Stevenson and Vancouver tidal gauges record relative sea level rise rates of 0.85–1.5 mm/yr since 1940 (Fig. 2). Local subsidence of the delta may account for an additional 2 mm/yr (Mazzotti et al., 2006). Long-term accretion rates measured with Cs-137 in marshes along Lulu Island, which neighbors Westham Island to the north, range from 2.6 mm/yr to 8.5 mm/yr (Williams and Hamilton, 1995). The lowest rates were measured near the

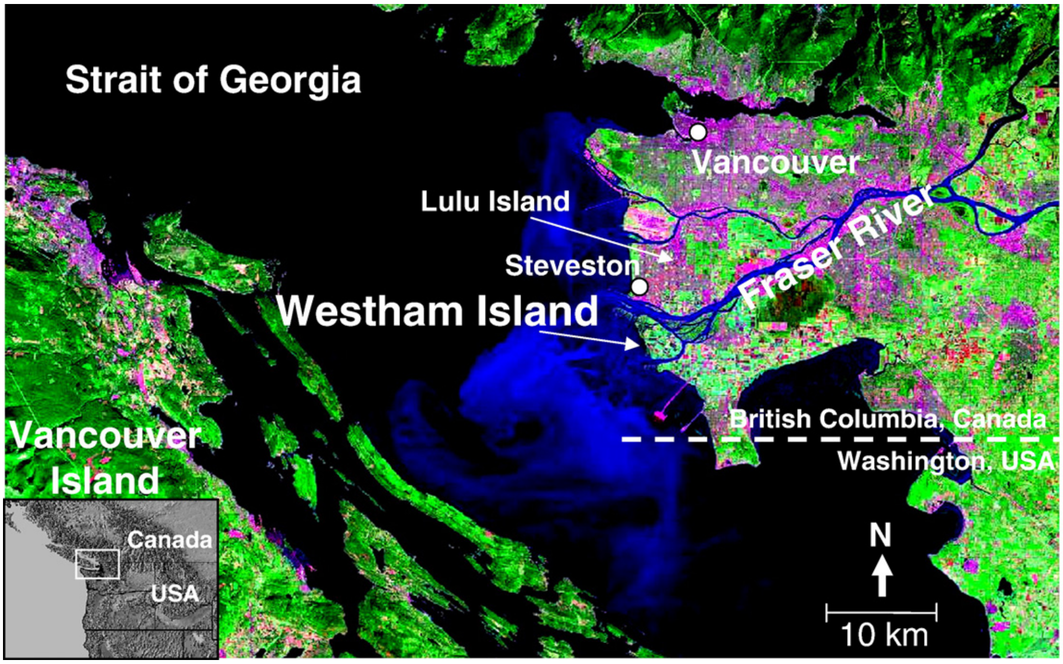

Fig. 1. Landsat image of Westham Island, British Columbia study area.

seaward border, likely reflecting the erosion or re-suspension of sediment by waves. Our coarse interpretation of historical photographs (1960s to present) suggests that the marsh has prograded seaward near channels, but is stable or slightly transgressing elsewhere.

3. Methods

3.1. Approach

We represent the topographic surface of Westham Island with a grid of elevation points determined by Light Detection and Ranging (LIDAR) in 2001, and resized to give a 5 × 5 m cell size (Fig. 4). The LIDAR elevations are relative to mean sea level. We measured water depth at several points on the marsh platform during a single spring high tide (July 22–23, 2005) and estimate that spring high tides inundate LIDAR elevations less than about 2.0 m. Our basic approach is to model local elevation change from vegetation-influenced deposition and a simplified treatment of wave erosion. At the end of each model iteration we calculate local deposition and erosion rates in every cell, and update the bed surface and sea level position. We then

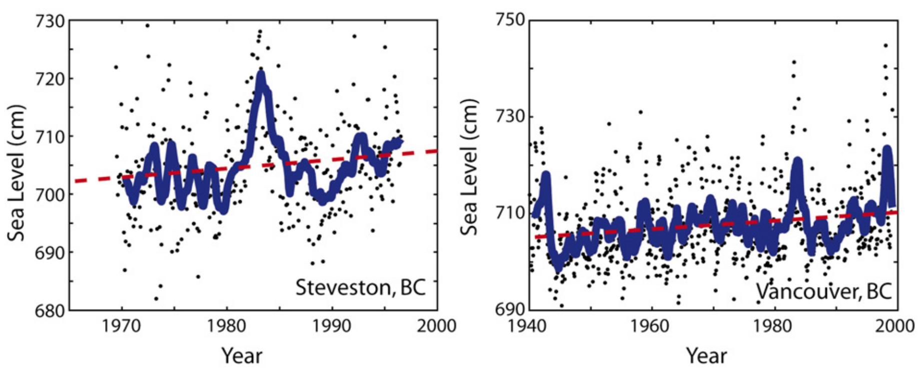

Fig. 2. Historical tidal gauge records of sea level near Westham Island. Steveston tidal gauge is 3 km and Vancouver tidal gauge is 17 km from Westham Island. Monthly sea level data (points) from PSMSL (2006), and has been smoothed with a 12-month moving average filter (solid line). Sea level rise rate determined by linear fit (dashed line) is 1.5 mm/yr and 0.85 mm/yr, respectively, at Steveston and Vancouver, British Columbia. Sea level plotted in reference to an arbitrary, global datum defined by PSMSL.

determine vegetation type and biomass productivity according to the bed surface elevation relative to sea level.

3.2. Deposition

Following Morris et al. (2002) and Kirwan and Murray (2007), the deposition rate in each cell depends on the concentration of sediment suspended above the marsh platform, C_{ss}, and the biomass productivity, B, of each cell:

$$\text{Deposition rate} = (q + k_2 * B) * h, \tag{1}$$

where q and k_2 are constants of proportionality (Morris et al., 2002). k_2 represents both the effect of sediment trapping by vegetation and the input of organic sediment, and q varies as a function of inorganic sediment supply. As in a number of previous aggradation models (e.g. French, 1993; Allen, 1995; Morris et al., 2002), the deposition rate is proportional to high tide water depth, h. We capture the basic behavior that suspended sediment concentrations decline with distance away from tidal channels by identifying the two major channels (Canoe Pass and the Main Arm of the Fraser River) that deliver sediment to Westham Island. In the model, we calculate values of q that exponentially decay with distance from these two major channels. While we expect the general form of this equation to hold in many inorganic dominated marshes, values of parameters q and k_2 depend on characteristics of a specific marsh and require local calibration (see Section 3.6).

3.3. Vegetation

The productivity and standing biomass of tidal marsh vegetation is related to the magnitude and frequency of tidal flooding (e.g. Reed and Cahoon, 1992). In previous morphological models (Morris et al., 2002; Mudd et al., 2004; Kirwan and Murray, 2005; D'Alpaos et al., 2007), vegetation productivity increases with inundation depth, up to some optimum depth. This relationship is based on a 20 yr record of *S. alterniflora* biomass productivity, a highly salt tolerant grass, in South Carolina, where annual variability in productivity correlates with mean annual sea level anomalies (Morris et al., 2002). At Westham Island, however, the marshes consist of multiple brackish-water species, and we observe that productivity generally declines with water depth. In the absence of a long-term dataset relating productivity to annual sea level, we measured biomass productivity and water depth along a transect from high to low marsh, and assume that a spatial relationship between productivity and depth is applicable to temporal changes in depth that may occur under increased rates of sea level rise. We measured the biomass of live stems along an elevation gradient in July, 2005 near the seasonal peak in standing biomass to estimate annual productivity (Giroux and Bedard, 1988). We sampled 12 25×25 cm quadrats at each elevation using the nondestructive methods of Thursby et al. (2002). Annual productivity of high marsh vegetation, dominated by *S. maritimus*, was approximately 600 g m^{-2} yr^{-1} (Fig. 3). This is significantly higher than the productivity of low marsh vegetation at Westham Island, which is dominated by *S. americanus* (Boyd, 1995). Karagatzides and Hutchinson (1991) also found that high elevation *S. maritimus* marsh was more productive than low *S. americanus* marsh on the Fraser River Delta. In the field, we observe a gradual rather than abrupt transition from *S. maritimus* to *S. americanus*, and assume that productivity decreases linearly in this transitional area. In the model, we assign a biomass productivity (B) based on the depth (h) of the bed surface below spring high tide sea level:

if	then	
$h < 1.1$	$B = 600$	(high marsh vegetation)
$1.1 \le h < 2.1$	$B = (600 - 400 * h)$	(transitional vegetation)
$2.1 \le h < 2.6$	$B = 200$	(low marsh vegetation)
$h \ge 2.6$	$B = 0$	(unvegetated tidal flats)

(2)

where B has units of g m^{-2} yr^{-1} and h has units of m.

3.4. Erosion

A variety of measurements of accretion and elevation change indicate that waves from the Georgia Strait erode

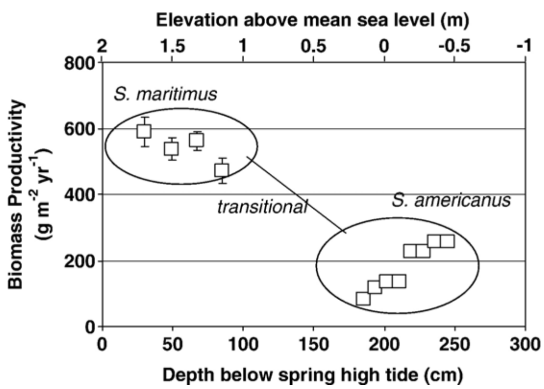

Fig. 3. Mean (±1 S.E.) biomass productivity of brackish marshes on Westham Island. Water depths were estimated from LIDAR elevations and measurements of water depth using the tide stick methodology of Smith and Warren (2007), during a spring high tide. *Scripus americanus* data from Boyd (1995).

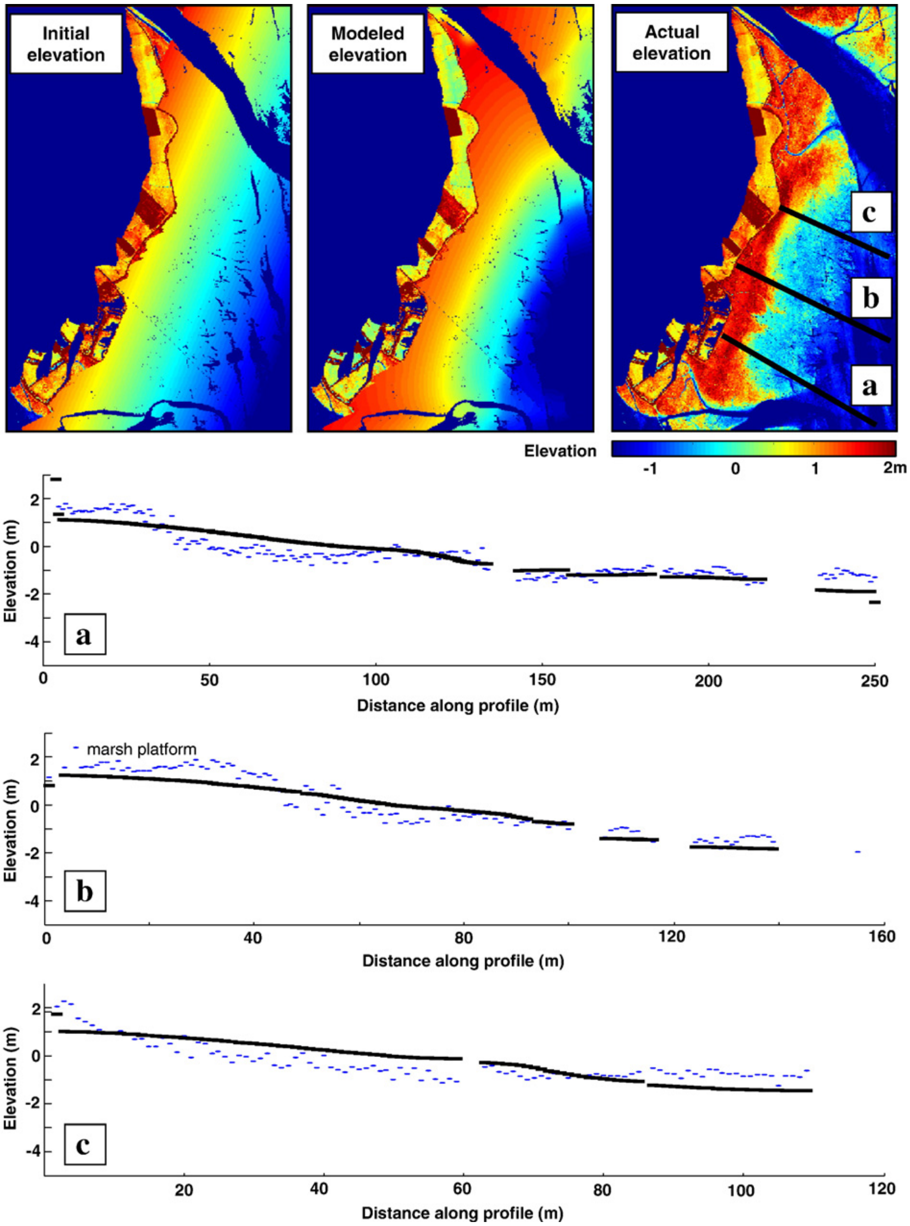

Fig. 4. Comparison between modeled topography and actual topography. Initial topography consisted of a constant slope. The modeled topography represents 2000 iterations (~330 yr) under 1 mm/yr sea level rise rate. Actual topography measured relative to mean sea level by LIDAR. In the profiles, modeled elevations are denoted by the heavy black line and actual elevations are denoted by the small blue points.

the surface of Fraser River Delta tidal flats and marshes (Boyd, 1995; Williams and Hamilton, 1995; Hill, 2006). In relatively deep water, a wave propagating landward tends to become taller as it moves into shallower water (shoaling). However, in relatively shallow water, bed friction and sediment entrainment attenuates wave heights as they propagate landward (Le Hir et al., 2000). At these water depths, representative of the upper reaches of tidal flats, attenuation due to bed friction is smaller when tides are high. Therefore, waves generally reach maximum heights during spring high tides. Following Le Hir et al. (2000), the maximum typical height of a wave in shallow water, H, is proportional to the depth of water, h, between the bed surface and sea level:

$$H = \gamma^* h. \tag{3}$$

Measurements of wave height and water depth typically indicate $\gamma \sim 0.15$ on tidal flats (e.g. Wells and Kemp, 1986; Le Hir et al., 2000). Similar values were measured on the Fraser River Delta flats from December 2003 through February 2004 (Houser, 2007 *personal communication*). This relationship is determined by continuously measuring wave heights at a single point in space over a period of time, typically including at least one spring-neap tidal cycle. While there is considerable scatter for lower wave heights, the highest waves for a given water depth exhibit a linear relationship with depth. Therefore, this proportionality yields the maximum wave height a tidal flat can experience at a given water depth. We use this temporal relationship between water depth and wave height to parameterize how wave heights dissipate as they move into shallower water.

Following Friedrichs and Aubrey (1996), velocities (U) at the bed of a mudflat in the model are related to wave height,

$$U = \frac{H}{2h}\sqrt{gh} \tag{4}$$

where g is the gravitational acceleration. We then use:

$$\tau_b = \frac{\rho f_w U^2}{8} \tag{5}$$

where f_w is a dimensionless friction factor (0.1), and ρ is the density of water, to estimate bed shear stress (Dean and Dalrymple, 1991). Fagherazzi and Furbish (2001) relate erosion rates to bed shear stress as:

$$\text{Erosion rate} = [m^*(\tau_b - \tau_c)/\tau_c]^*\delta. \tag{6}$$

For cohesive mud, Fagherazzi and Furbish (2001) suggest that m is a constant (0.0014 kg m^{-2} s^{-1}) and τ_c represents a threshold shear stress (0.4 N m^{-2}) below which no erosion occurs. We acknowledge that vegetation attenuates wave heights and increases the shear strength of sediments. In this initial modeling exercise we do not account for these details but will incorporate them into more elaborate versions of the model in the future.

Furthermore, we calculate only a maximum wave height for each bed elevation in the model domain, and assume that this wave height is the most effective one for erosion. Therefore, we multiply the erosion rate by a dimensionless parameter, δ, to represent both the effect of smaller waves and the intermittency of large waves ($\delta \sim 100$, see Appendix A).

3.5. Topographic smoothing and model time step

During each model iteration the net erosion and deposition that takes place during a complete (12 h) tidal cycle is calculated. We do not address temporal variations in sediment transport within a tidal cycle. At the end of each iteration, we smooth the topographic bed surface by calculating small fluxes of sediment that move downslope due to gravity-driven processes (e.g. topographic diffusion). The flux into each cell is proportional to the slope to its neighbors, and inversely proportional to biomass productivity, reflecting the stabilizing character of plant roots (Kirwan and Murray, 2007). All changes in bed elevation and productivity are calculated at the end of each iteration and, assuming 2 tidal cycles per day, multiplied by 120 to give a model time step of 2 months. We therefore do not consider daily or seasonal variation in tide height or sediment transport, consistent with our goal of exploring the basic responses of marshes to long-term sea level change.

3.6. Model calibration

Water depths at one location on an intertidal surface remain constant when the net accretion rate (deposition minus erosion) equals the sea level rise rate. For a given rate of sea level rise, Morris et al. (2002) explains that this equilibrium water depth is a function of the sediment supply and biomass productivity. Morris et al. (2002) used fertilization experiments and a 20 yr record of productivity to parameterize the local relationships between water depth, deposition, and productivity in their South Carolina salt marsh. In the absence of such long-term data at Westham Island, we use knowledge of the intertidal surface topography, and an assumption that portions of the intertidal surfaces are nearly in equilibrium with long-term rates of sea level rise, to solve Eqs. (1) and (6) in order to estimate the deposition and erosion related parameters (Appendix A).

In an effort to determine whether we have incorporated the most important processes and chosen reasonable parameter values, we modeled the development of intertidal surfaces under the historic rate of sea level rise and compared it to the observed modern topography. The model simulation began with an arbitrary surface of constant slope (Fig. 4). Rapid deposition in the upper portions of the marsh caused water depths to shallow towards the high marsh equilibrium depth. Erosion rates that increased with depth led to a concave profile in the lower marsh and tidal flats. Progradation of the marsh surface was greatest near the major channels, reflecting a spatially variable suspended sediment concentration.

Although the model cannot capture small-scale heterogeneity in the marsh and flat morphology, modeled elevations generally resemble measured elevations (Fig. 4). These similarities suggest that despite a number of simplifying assumptions, we have captured the essential characteristics of the most important processes acting on Westham Island.

4. Model experiments

Using the LIDAR determined elevations as an initial topographic surface, we modeled the response over 100 yr of Westham Island to several sea level scenarios summarized in the Intergovernmental Panel on Climate Change report (IPCC, 2001; IPCC, 2007). We used the lowest and highest sea level scenarios from the full range of all AOGCMs to force our "low" and "high" sea level experiments, and the IPCC (A1F1) scenario to force our "median" sea level experiment (IPCC, 2001). For each scenario, we estimated sea level positions at 2000, 2030, 2050, and 2100 and interpolated a linear rate of rise in between these years (Fig. 8). Sea level positions were visually estimated from Figure 11.12 in the IPCC, except for the positions at 2100 which are reported in the text (IPCC, 2001). More recent synthesis suggests nearly identical rates of sea level rise (IPCC, 2007), though projections of extreme sea level rise resulting from rapid changes in ice flow were not included (e.g. Alley et al., 2005; Vaughan, in press). Sea level predictions listed in the IPCC begin in 1990. Since our simulations begin from 2000, we subtract the IPCC sea level position at 2000 prior to determining any future sea level position or rate of rise.

While the IPCC scenarios forecast eustatic sea level change, processes including glacial rebound, tectonic uplift, and subsidence may influence local, relative sea level rise rates (e.g. Long and Shennan, 1998). In particular, approximately eight episodes of rapid marsh

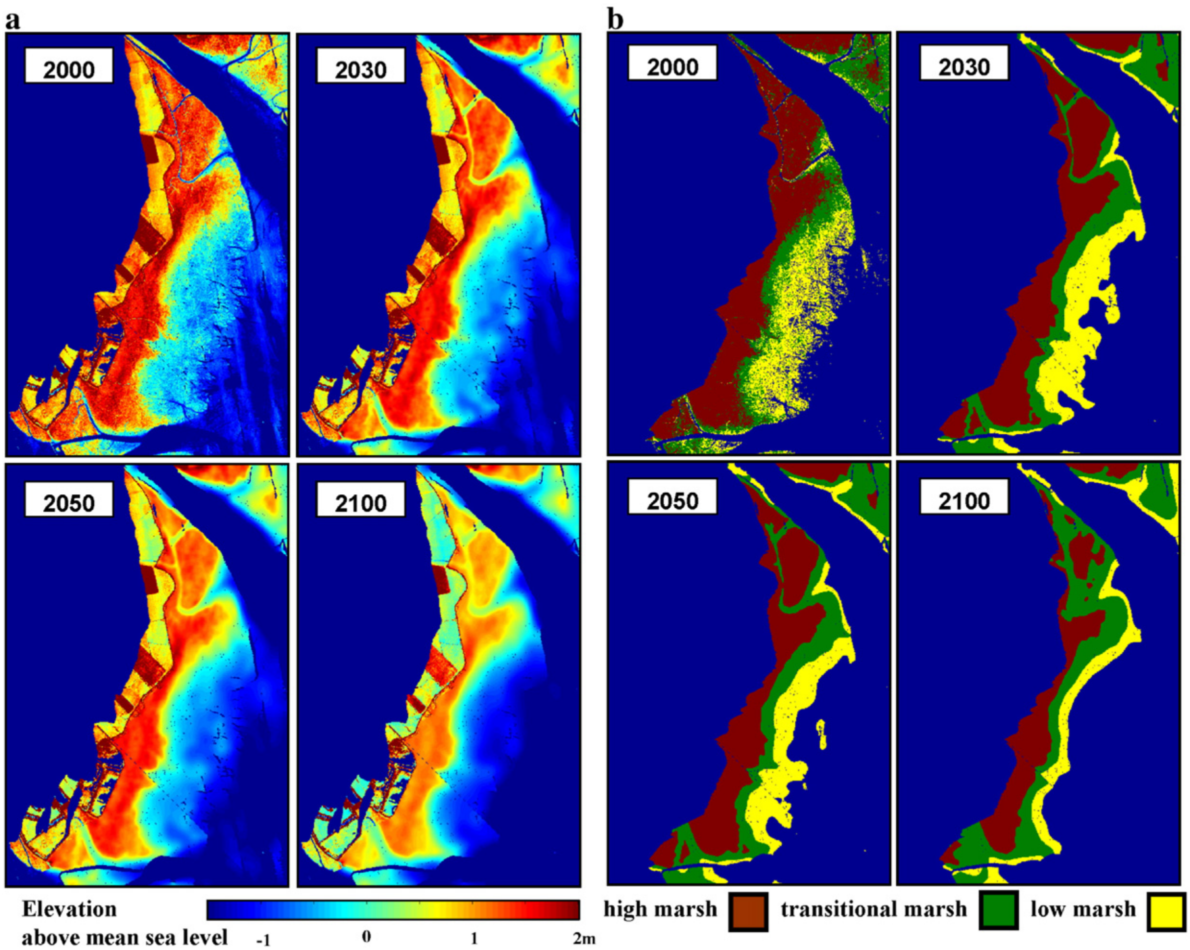

Fig. 5. Maps of bed elevations (a) and vegetation zones (b) modeled in response to median sea level rise scenario adjusted for local rate of subsidence.

submergence, associated with seismic events, have occurred in the last 5000 yr elsewhere in the region (e.g. Long and Shennan, 1998). We assume these episodes occur on a longer time scale, and do not account for them in our estimates of next-century sea level rise. Moreover, Late Holocene estimates of eustatic sea level rise of ~1 mm/yr (e.g. Donnelly et al., 2004), are similar to both historical rates at nearby tidal gauges (Fig. 2), and long-term sea level reconstructions from elsewhere in the region (Long and Shennan, 1998), suggesting that eustatic projections are generally applicable to this area. Recent high-precision GPS measurements and geodetic leveling suggest the land surface of the delta is subsiding 1–3 mm/yr (Mazzotti et al., 2006). Therefore, we pair eustatic model simulations with experiments in which we add 2 mm/yr to the sea level forecasts to represent local, relative sea level rise. These paired experiments allow us to model the response of a marsh to both relative and eustatic sea level change, and provide some measure of model sensitivity to sea level rise rates.

5. Results

The marshes and tidal flats of Westham Island deepened in response to median and high sea level rise scenarios (Figs. 5a, 6a). Accretion tended to increase the elevation of the high marsh, but not as rapidly as the rate of sea level rise. Wave erosion tended to decrease the elevation of low marshes and tidal flats, resulting in water depth increases that were greater than the rate of sea level rise. Deepening bed surfaces caused marsh zones to migrate landward, with low marsh vegetation replacing transitional zone vegetation, and transitional vegetation replacing high marsh vegetation (Figs. 5b, 6b). The dyke along the marsh's landward boundary prevented high marsh vegetation from migrating landward.

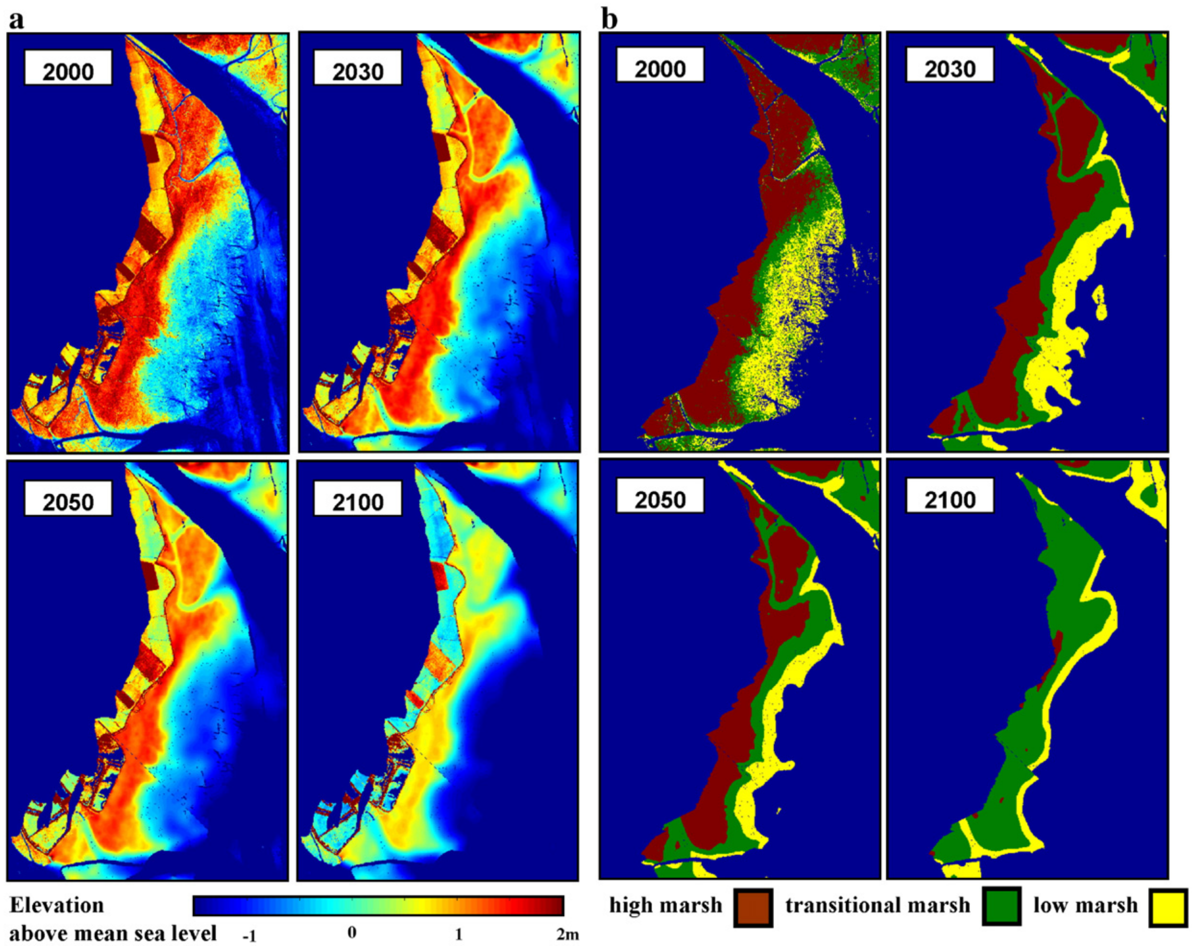

Fig. 6. Maps of bed elevations (a) and vegetation zones (b) modeled in response to high sea level rise scenario adjusted for local rate of subsidence.

The majority of marsh converted to open water was in the low marsh fringe where wave erosion rates were high. Virtually the entire discontinuous low marsh fringe converted to open water, even at median sea level scenarios. Conversely, marsh tended to persist, even at the highest rates of sea level rise, near channels where initial topography and suspended sediment concentrations were high. These marshes did lose elevation relative to sea level, indicating that suspended sediment concentrations and rapid vegetation productivity in the high marsh were insufficient to offset accelerating sea level rise. Consequently, transitional zone marsh vegetation replaced large areas of high marsh vegetation near the channels.

At relatively low rates of sea level rise, accretion exceeded sea level rise, leading to progradation of the bed surface, and expansion of the marsh onto previously unvegetated tidal flats. Under most sea level scenarios, progradation was limited to the first 10 yr of sea level rise (Fig. 7). However, in the low eustatic scenario (i.e. without subsidence), progradation resulted in long-term net expansion of the high marsh and transitional zones, despite 100 yr of sea level rise (Table 1).

5.1. Low sea level scenarios

Under low sea level rise scenarios, the water depth averaged across all Westham Island surfaces was approximately unchanged despite 100 yr of sea level rise. The total area covered by high marsh vegetation was similarly relatively stable. Transitional zone vegetation expanded primarily in the seaward direction (though also slightly landward) by a total of 6–10%. Low marsh vegetation decreased by 1–15% (1% without local subsidence effects, 15% when subsidence is included), the majority of which was lost due to submergence of the bed surface rather than replacement by the seaward expansion of transitional zone marsh. (We do not include figures of elevation and vegetation change because their responses were so slight.)

5.2. Median sea level scenarios

Under median sea level rise scenarios, mean water depth at Westham Island increased by about 35–55 cm in response to a total sea level change of about 45–65 cm by the year 2100. Deepening resulted in a loss of intertidal area covered by vegetation of about 20% (800,000 m^2 for median scenario without subsidence). High marsh vegetation coverage decreased 25–50% and low marsh vegetation decreased by 30–35% (Table 1, Fig. 7). Transitional zone marsh vegetation migrated landward, expanding the area of intertidal surfaces covered by transitional vegetation by about 10–20%. A total of 800,000 m^2 of initially low marsh was converted to open water (Appendix B). Since the area of low marsh converted to open water closely resembles the total amount of vegetated area lost, we conclude that loss of vegetated surfaces took place entirely in the low marsh zone.

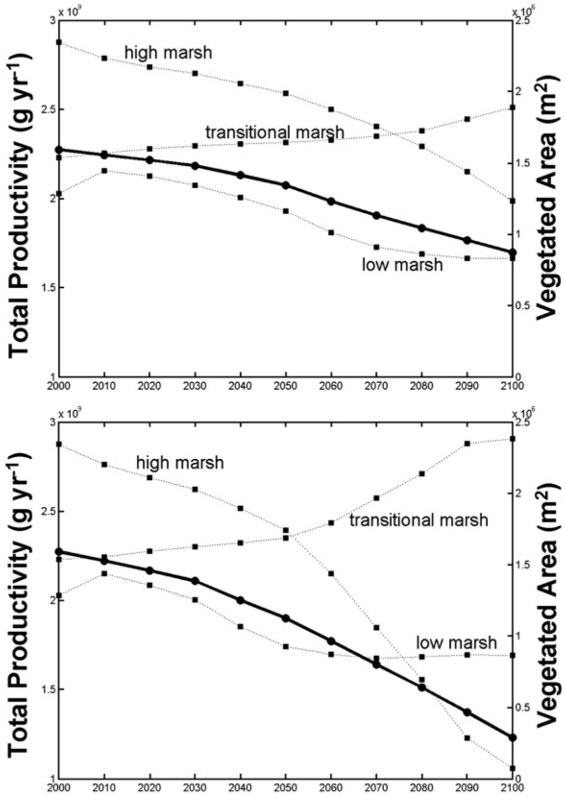

Fig. 7. Response of vegetation to 100 yr of sea level rise. Top graph shows response to median sea level scenario adjusted for local subsidence rate, bottom graph shows response to high sea level scenario adjusted for local subsidence rate. Heavy solid line denotes total annual productivity at Westham Island. Dotted lines denote the area of surfaces covered by high, low, and transitional marsh vegetation.

5.3. High sea level scenarios

Under high sea level rise scenarios, mean water depth increased by about 70–90 cm in response to a sea level change of about 80–100 cm. Deepening resulted in a 30–35% loss of vegetated area, nearly all of which occurred on surfaces previously covered by low marsh vegetation. The area covered by high marsh vegetation declined 75–95%, with remaining patches of high marsh vegetation restricted to isolated areas with extremely high initial elevations (Fig. 6). The high marsh was replaced by transitional zone vegetation which

Table 1
Changes to Westham Island after 100 yr of sea level rise

Scenario	Low	Low*	Med	Med*	High	High*
Sea level rise (m)	.079	.276	.454	.651	.839	1.036
Depth change (m)	−.026	.165	.338	.534	.719	.915
Total biomass (% change)	5	−6	−16	−25	−35	−46
Vegetated area (% change)	4	−6	−16	−23	−30	−36
High marsh	4	−9	−24	−47	−76	−97
Transition	10	6	10	23	45	55
Low marsh	−1	−15	−31	−35	−34	−33
Vegetated area (change, m^2)	213,375	−310,975	−812,975	−1,211,275	−1,525,800	−1,846,425
High marsh	82,500	−214,200	−558,800	−1,109,325	−1,779,775	−2,270,825
Transition	147,400	92,650	150,375	352,975	685,050	845,600
Low marsh	−16,525	−189,425	−404,550	−454,925	−431,075	−421,200

Asterisks denote sea level scenarios adjusted for local rates of subsidence. Depth change measures the increase in high-tide water depth above the depth of the bed (positive numbers denote increase in water depth). Losses in total biomass or vegetated area denoted by negative numbers.

expanded its coverage by 45–55%. Loss of vegetated surface area took place exclusively in the low marsh, and surfaces initially covered by transitional and high marsh vegetation remained vegetated.

In all median and high sea level scenarios, low marsh was able to migrate landward. However, net loss of low marsh indicates that, on average, seaward erosion outpaced landward migration of the low marsh zone (see Appendix B for details). The 100 yr loss of low marsh vegetation is equivalent under high and median sea level scenarios, while the loss of total vegetated area is much greater under high sea level scenarios. This indicates that the seaward edge of the low marsh must migrate faster under high sea level rise rates. During the highest rates of sea level rise (the last 40 yr of the high scenarios), the area of low marsh does not change indicating that seaward and landward edges migrate at the same rate.

5.4. Synthesis of response to different sea level scenarios

Loss of vegetated area and loss of total biomass productivity generally mimic each other (Table 1) indicating that the majority of productivity lost was due to conversion of low marsh to open water. While less productive transitional zone vegetation did replace more highly productive high marsh vegetation, and low marsh replaced transitional marsh, this process only minimally affected total biomass production. Only in the highest sea level scenarios did deepening of marsh zones appear significant, resulting in a decrease of total productivity by an additional 5–10% after 100 yr.

The rate of change of bed surfaces and the vegetation that colonizes them is not constant through time. Sea level accelerates through time, and patterns of vegetation change generally follow that acceleration. For example, high marsh vegetation loss and transitional vegetation expansion is more rapid after 2050 (Fig. 7). Low marsh vegetation zones expand seaward for the first 10 yr and then erode at progressively higher rates until about 2050 or 2060, depending on the sea level scenario. For the next 20 yr the rate of low marsh loss begins to stabilize, and the total area of low marsh remains constant after about 2070–2080. The total area of surfaces covered by vegetation follows a similar temporal pattern (Fig. 8). The loss rate of vegetated area increases immediately following sea level rise rate increases at 2030 and 2050, and then begins to stabilize after about 2060. In the median sea level scenario, biomass productivity mimics total vegetated area throughout the 100 yr simulation (Fig. 8a). In the high sea level scenario, however, the amount of productivity lost diverges from the amount of vegetated area lost after 2060 (Fig. 8b). More specifically, the loss rate of biomass productivity continues to increase, even though the loss rate of vegetated area remains constant or slows slightly. The tendency for less productive vegetation, characteristic of lower surfaces, to replace highly productive vegetation, characteristic of shallow surfaces, explains this divergence. The divergence is only apparent at the end of the most rapid sea level scenarios where the total area of vegetated surfaces is low and the rate of zone migration is high.

6. Discussion

In this initial exploratory model, we have intentionally treated a number of biological and sediment transport processes in highly simplified ways. This approach allows simulation over large spatial and temporal scales, and tends to maximize the clarity of results, but is not

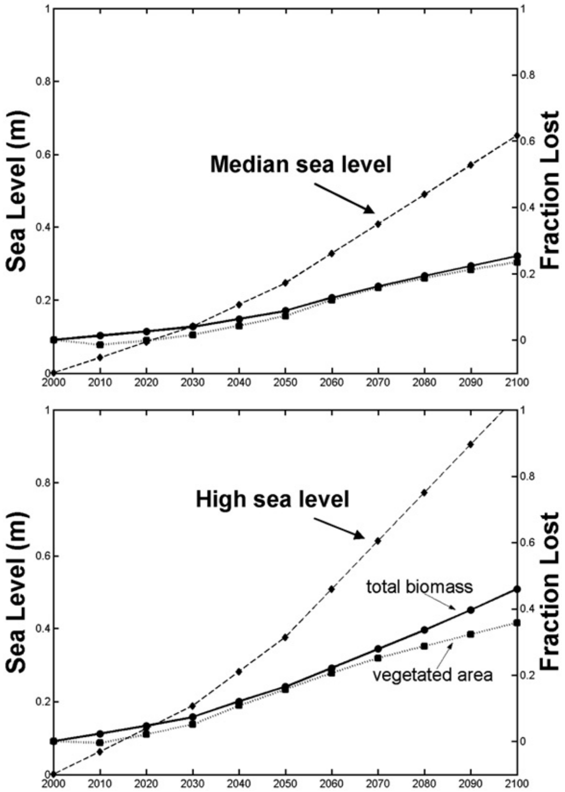

Fig. 8. Response of vegetation to 100 yr of sea level rise. (a) Response to median sea level scenario adjusted for local rates of subsidence. Fraction of vegetated area lost (solid line, square markers) closely resembles fraction of biomass productivity lost (dotted line, circle markers). Both vegetated area and biomass productivity begin to stabilize after about 2060. (b) Response to high sea level scenario adjusted for local rates of subsidence). Fraction of vegetated area lost closely resembles fraction of biomass productivity lost until about 2060. After 2060, the vegetated area begins to stabilize, but the rate of loss biomass productivity continues to increase.

necessarily appropriate for making precise and detailed predictions (Murray, 2003). For example, we measured biomass productivity across a spatial gradient to formulate how biomass productivity will respond to temporal changes in water depth. In reality, factors other than water depth affect productivity along the spatial gradient. Our simplified treatment of wave attenuation will not likely predict quantitatively accurate wave-induced water velocities. Instead, we rely on the dimensionless parameter, δ, to obtain realistic erosion rates. The accuracy of both depositional and erosional parameter values depends on the ability to select accurate equilibrium depths from the marsh topography. In reality, intertidal surfaces today are likely evolving towards new equilibrium depths due to sediment diversion, vegetation disturbance, and possible relative sea level rise rate change. Equilibrium depths, even if they could be identified more reliably, may partially reflect modern conditions rather than the long-term conditions we assume the marshes and flats developed under. Our model results should then be interpreted as a preliminary exploration of how broad morphology and vegetation patterns respond to future sea level scenarios rather than detailed quantitative predictions.

Despite a number of simplifying assumptions, our model produces topography similar to that measured by LIDAR. Modeled behavior also agrees qualitatively with behavior observed in the geologic record. For example, Williams and Roberts (1989) demonstrated with stratigraphic cross sections and radiocarbon analysis that the Fraser River Delta prograded seaward throughout its 9000 yr history, even during periods of sea level acceleration and moderately high rates of sea level rise. In their sediment cores, marsh and tidal flat facies overlie coarser sands across the entire delta, suggesting that the delta responded to increased rates of sea level rise with a depositional regression rather than a marine transgression. In the early stages of all our model simulations, and throughout the slowest sea level scenario, we similarly observe a prograding delta and seaward regression of marsh zonation.

Marshes on Lulu Island, which neighbors Westham Island to the North, accreted at an average rate of 2.6–8.5 mm/yr between 1964 and 1991 (Williams and Hamilton, 1995). Given a subsidence rate of 2 mm/yr and a sea level rise rate of about 1 mm/yr, this suggests that the marsh generally maintained or increased its elevation relative to sea level since 1964. While vertical accretion rates that exceed relative sea level rise rates do not necessarily indicate lateral delta progradation (the marsh could simply build in the vertical direction), they do indicate that this part of the delta did not transgress landward since 1964. Either way, these historical accretion rates are generally consistent with our model prediction that marine transgression and landward migration of vegetation zones will not occur under present day conditions or slow future sea level scenarios.

Because the high accretion rates on Lulu Island are long-term averages, it is possible that accretion has been slower than relative sea level rise in recent years, and that intertidal surfaces have deepened. Williams and Hamilton (1995) suggest that accretion rates have declined. For example, low marsh accretion rates were 6 mm/yr between 1954–1964, and only 3 mm/yr from 1964–1991 (Williams and Hamilton, 1995). Short term measurements of bed surface elevation (1990–1992) indicate that where low marsh vegetation is disturbed by geese, the bed is actually eroding (as opposed to slow accretion) by about 1 cm/yr (Boyd, 1995). Large pedestals of marsh are surrounded by unvegetated tidal flats at both Lulu and Westham Islands. Given that the pedestals are on the order of 50 cm high, and given that the surrounding surfaces disturbed by geese erode at 1 cm/yr, we estimate that the pedestals formed within approximately the last 50 yr. These geomorphic and stratigraphic observations suggest that deepening of tidal surfaces on the Fraser River Delta are a recent phenomena. If sea level accelerates according to the IPCC future scenarios, then our model predicts a marine transgression and landward migration of vegetation zones that is historically unprecedented, at least in this region.

The dyke along the upper border of the high marsh prevents vegetation from migrating landward with sea level acceleration. While our model experiments suggest that the high marsh will largely maintain its position under slow sea level scenarios, transitional zone vegetation migrates landward under median and high sea level scenarios, resulting in loss of high marsh. Because the lower extent of the low marsh moves landward in all IPCC scenarios, migration of vegetation zones results in a net loss of marshland. If the high marsh were able to expand into higher elevations at a rate (area/yr) equal to the rate of low marsh converted to open water, then the total marsh area (and approximately the total biomass productivity) would maintain an equilibrium with sea level. However, under the median sea level scenario, 800,000 m^2 of low marsh converts to open water while losses of high marsh approximate 550,000 m^2. If in the absence of a dyke, high marsh vegetation were displaced (i.e. migrating landward) rather than replaced by transitional zone vegetation, marsh loss would still total about 250,000 m^2. Therefore, our model simulations suggest that the dyke is responsible for 70% of marsh loss under the median sea level scenario. Under more rapid sea level scenarios, high marsh vegetation migrates more rapidly than the rate at which low marsh converts to open water, suggesting that migration in the absence of a dyke would make up for marsh lost at the seaward edge.

Because the IPCC scenarios predict an increasing rate of sea level rise, and because relationships between sea level and vegetation are nonlinear, there is considerable temporal variability in vegetation patterns. For example, rates of change are generally greater after 2050, suggesting that predictions based on short term model simulations and field measurements made in the next decades may underestimate change. On the other hand, specific components of the system (i.e. the rate of low marsh loss) may stabilize in the long-term, leading to overestimations of change in these parts of the system that are based on short term observations. Our model simulations indicate that trends in vegetated area and total biomass productivity generally mimic each other at Westham Island under low rates of sea level rise, but diverge at higher rates after 2060. This suggests that observations of a stable vegetated area would potentially neglect a loss of productivity at high rates of sea level rise. Existing numerical models that simulate how a specific marsh landscape responds to sea level change have been run approximately 20–50 yr into the future (e.g. Reyes et al., 2000; Martin et al., 2002). Our model simulations predict that important changes in behavior take place after about 2050, suggesting that predictions based on short term modeling and future field measurements may not adequately represent long-term behavior.

7. Conclusions

Simplifying assumptions and poorly constrained parameter calibration clearly make this an exploratory type model, not well suited for making precise, quantitative predictions about the response of Westham Island to future sea level scenarios. However, the incorporation of several key processes and the ability to simulate long-term behavior allow the model to provide several fundamental insights into the response of marshes and tidal flats to sea level rise:

1. Under present day and slow future sea level scenarios, the marshes at Westham Island should be able to maintain their morphology and vegetation characteristics.
2. Our model predicts that under more rapid scenarios of future sea level rise, vegetation will migrate landward and lead to a loss of biomass productivity, with greatest rates of loss occurring far from channels.
3. The reduction in biomass productivity is almost entirely due to loss of vegetated area, though replacement of highly productive vegetation with less productive vegetation is significant under more rapid scenarios of sea level rise.
4. The inability of marshes to migrate beyond the dyke accounts for most of future marsh loss under median sea level scenarios.
5. Several important changes in marsh behavior take place after about 2050, suggesting that predictions based on short term observations may not accurately reflect long-term behavior.

Acknowledgements

We appreciate the continued assistance of Sean Boyd, Phil Hill, Chris Houser, and Alex Shaw throughout the project. Peter Kirwan helped with field and lab work. The Geological Survey of Canada and the US National Science Foundation (EAR 1617209) supported the work.

Appendix A. Model calibration

Expansive marsh platforms with high and topographically flat elevations characterize the Westham Island marshes near channels. These characteristics, combined with observations of general channel and platform edge stability in historical photographs, suggest that this portion of Westham Island is close to being in equilibrium with sea level. These marshes generally have a well defined marsh platform with an elevation of about 1.7 m above mean sea level (see profile B, Fig. 4). Measurements taken during a spring high tide suggest maximum water depths of about 0.3 m above the high marsh platform. If we assume the broad platform represents an equilibrium surface, and assume negligible wave erosion in the high marsh, then the deposition rate must equal the long-term sea level rise rate at a water depth of 0.3 m. Eq. (1) may then be solved to estimate parameters q and k_2.

$$\text{Deposition rate} = (q + k_2{*}B){*}h. \quad (1)$$

In the late Holocene, eustatic sea level rose about 1 mm/yr, roughly consistent with local short term tidal gauge records (i.e. Fig. 2). Since biomass productivity in the high marsh equals ~600 g m^{-2} yr^{-1}, Eq. (1) becomes:

$$1\text{E} - 3 \text{ m yr}^{-1} = [q + (600 \text{ g m}^2\text{yr}^{-1}{*}k_2)]{*}0.3\text{m}.$$

Rearranging yields k_2=(.0033 yr$^{-1}-q$)/600 g m^{-2} yr^{-1}. Of these two remaining variables, k_2 probably varies most as a function of local conditions and vegetation type, while q can be roughly estimated using local measurements. Following Morris et al. (2002), the value of q depends on the suspended sediment concentration, SSC, which Kirwan and Murray (2007) expressed as $q=k_1*$ SSC where k_1=9E−5 m^3 g^{-1} yr^{-1}. The Vancouver Port Authority (2005) reports suspended sediment concentrations at 10 monitoring sites, measured monthly during high tides from May–October, 2004, on the tidal flats along the Fraser River Delta. Near the major channels, concentrations are on the order of 10 g m^{-3} yielding q=9E−4 yr^{-1}, and k_2=4.05E−6 m^2 g^{-1}. Despite a number of assumptions and lack of long-term measurements, our estimate of k_2 resembles Morris et al.'s (2002) estimate of 1.5E−5 m^2 g^{-1} based on long-term field experiments. Differences in vegetation type and physical characteristics of the two locations likely explain the difference.

The Westham Island tidal flats generally become topographically level at an elevation of about 1 m below mean sea level (~3 m spring high tide water depth). Using similar methods, we can estimate the value of δ if we assume that tidal flats at depths of ~3 m represent another equilibrium surface. In this case, deposition must balance the effects of sea level rise and erosion in order to achieve equilibrium. Therefore the long-term erosion rate equals the deposition rate minus the sea level rise rate:

$$[m{*}(\tau_b - \tau_c)/\tau_c]{*}\delta = [(q + k_2{*}B){*}h] - 1\text{E} - 3 \text{ m yr}^{-1}.$$

Biomass productivity (B) at 3 m depth equals zero, yielding deposition=3*q or 2.7E−3 m yr^{-1}. Therefore, the long-term erosion rate of waves eroding the bed at a depth of 3 m must equal 1.7E−3 m yr^{-1} (2.7E−3 m yr^{-1}−1E−3 m yr^{-1}). When h=3.0 and H=1.0, $[m*(\tau_b-\tau_c)/\tau_c]$=1.4E−5 m s^{-1}, representing a short-term erosion rate for large waves. To achieve long-term erosion rates that maintain equilibrium water depth, the dimensionless parameter, δ, must equal ~100.

Appendix B. Result details

B.1. Median sea level scenarios

In the model, we do not directly calculate the area of low marsh converted to open water. Instead, we determine the area of low marsh converted to open water by a series of calculations involving the change in area of the various vegetation zones. For example, if low marsh was unable to migrate landward, transitional marsh coverage would be expected to expand by an amount equal to the loss of high marsh. However, high marsh loss totaled ~550,000 m^2 while transitional marsh expanded only 150,000 m^2 (Table 1). Therefore, 400,000 m^2 of surfaces initially covered by transitional vegetation must have been replaced by low marsh migrating landward. Surfaces covered by low marsh constricted 400,000 m^2, meaning that a total of 800,000 m^2 of initially low marsh must have been converted to open water (low marsh converted to open water=initial low marsh−(final low marsh−created low marsh)). Since the area of low marsh converted to open water closely resembles the total amount of vegetated area lost, we conclude that all loss of vegetated surfaces took place in the low marsh.

B.2. High sea level scenarios

The area covered by high marsh vegetation declined by 1,800,000–2,200,000 m^2. The high marsh was replaced by transitional zone vegetation which expanded its coverage by 690,000–890,000 m^2. Low marsh therefore replaced about 1,100,000–1,300,000 m^2 of the transitional zone vegetation. Since the total area of low marsh declined 410,000–430,000 m^2 (Table 1), approximately 1,500,000–1,700,000 m^2 of low marsh must have converted to open water.

References

Allen, J.R.L., 1995. Salt marsh growth and Flandrian sea level: implication of a simulation model for Flandrian coastal stratigraphy and peat-based sea-level curves. Sedimentary Geology 100, 21–45.

Allen, J.R.L., 1997. Simulation models of salt-marsh morphodynamics: some implications for high-interval sediment couplets related to sea-level change. Sedimentary Geology 113, 211–223.

Alley, R.B., Clark, P.U., Huybrechts, P., Joughin, I., 2005. Ice-sheet and sea-level changes. Science 310, 456–460.

Boyd, W.S., 1995. Lesser snow geese (*Anser c. caerulescens*) and American three-square bulrush (*Scirpus americanus*) on the Fraser and Skagit river deltas. Ph.D. Thesis, Simon Fraser University, Burnaby, Canada. 154 pp.

Brinson, M.M., Bradshaw, H.D., Jones, M.N., 1985. Transitions in forested wetlands along gradients of salinity and hydroperiod. Journal of the Elisha Mitchell Science Society 101, 76–94.

Canadian Hydrographic Service, 2006. Tides, Currents, and Water Levels. http://www.waterlevels.gc.ca.

Costanza, R., d'Arge, R., de Groot, R., Farber, S., Grasso, M., Hannon, B., Limburg, K., Naeem, S., O'Neil, R.V., Paruelo, J., Raskin, R.G., Sutton, P., van den Belt, M., 1997. The value of the world's ecosystem services and natural capital. Nature 387, 253–260.

D'Alpaos, A., Lanzoni, S., Marani, M., Rinaldo, A., 2007. Landscape evolution in tidal embayments: modeling the interplay of erosion, sedimentation, and vegetation dynamics. Journal of Geophysical Research 112. doi:10.1029/2006JF000537.

Dean, R.G., Dalrymple, R.A., 1991. Water wave mechanics for engineers and scientists. Advanced Series on Ocean Engineering, vol. 2. World Scientific Publishing Company, New Jersey. 353 p.

Donnelly, J.P., Cleary, P., Newby, P., Ettinger, R., 2004. Coupling instrumental and geological records of sea-level change: evidence from southern New England of an increase in the rate of sea-level rise in the late 19th century. Geophysical Research Letters 31, L05203. doi:10.1029/2003GL018933.

Fagherazzi, S., Furbish, D.J., 2001. On the shape and widening of salt marsh creeks. Journal of Geophysical Research 106, 991–1003.

French, J.R., 1993. Numerical simulation of vertical marsh growth and adjustment to accelerated sea-level rise, North Norfolk, UK. Earth Surface Processes and Landforms 18, 63–81.

Friedrichs, C.T., Aubrey, D.G., 1996. Uniform bottom shear stress and equilibrium hyposometry of intertidal flats. In: Pattiaratchi, C. (Ed.), Mixing in Estuaries and Coastal Seas. American Geophysical Union, Washington, D.C., pp. 405–429.

Friedrichs, C.T., Perry, J.E., 2001. Tidal salt marsh morphodynamics: a synthesis. Journal of Coastal Research 27, 7–37.

Giroux, J.F., Bedard, J., 1988. Estimating above-and below-ground macrophyte production in *Scirpus* tidal marshes. Canadian Journal of Botany 66, 368–374.

Hartig, E.K., Gornitz, V., Kolker, A., Mushacke, F., Fallon, D., 2002. Anthropogenic and climate-change impacts on salt marshes of Jamaica Bay, New York City. Wetlands 22, 71–89.

Hill, P.R. (ed.), 2006. Biophysical impacts of sea level rise and changing storm conditions on Roberts Bank. Draft Assessment Report. Geological Survey of Canada, Unpublished Report, 42 pp.

Houser, C., 2007. Personal communication. University of West Florida Coastal Morphodynamics and Sediment Transport Group.

IPCC (Intergovernmental Panel on Climate Change), 2001. Climate change 2001: the scientific basis. Contribution of Working Group I to the Third Assessment Report of the IPCC. Cambridge University Press, Cambridge, UK. 881 pp.

IPCC (Intergovernmental Panel on Climate Change), 2007. Climate change 2007: the physical science basis, summary for policy makers. Contribution of Working Group I to the Fourth Assessment Report of the IPCC. Cambridge University Press, Cambridge, UK. 18 pp.

Karagatzides, J.D., Hutchinson, I., 1991. Intraspecific comparisons of biomass dynamics in *Scirpus americanus* and *Scirpus maritimus* on the Fraser River Delta. The Journal of Ecology 79, 459–476.

Kearney, M.S., Rogers, A.S., Towshend, G., Rizzo, E., Stutzer, D., 2002. Landsat imagery shows decline of coastal marshes in Chesapeake and Delaware Bays. EOS Transactions 83, 173–178.

Kirwan, M.L., Murray, A.B., 2005. Response of an ecomorphodynamic model of tidal marshes to varying sea level rise rates. In: Parker, G., Garcia, M.H. (Eds.), River, Coastal, and Estuarine Morphodynamics: RCEM 2005, vol. 2, pp. 629–634.

Kirwan, M.L., Murray, A.B., 2007. A coupled geomorphic and ecological model of tidal marsh evolution. Proceedings of the National Academy of Sciences 104, 6118–6122.

Kirwan, M.L., Kirwan, J.L., Copenheaver, C.A., 2007. Dynamics of an estuarine forest and its response to rising sea level. Journal of Coastal Research 23, 457–463.

Le Hir, P., Roberts, W., Cazaillet, O., Christie, M., Bassoullet, P., Bacher, C., 2000. Characterization of intertidal flat hydrodynamics. Continental Shelf Research 20, 1433–1459.

Long, A.J., Shennan, I., 1998. Models of rapid relative sea-level change in Washington and Oregon, USA. The Holocene 8, 129–142.

Martin, J.F., Reyes, E., Kemp, G.P., Mashriqui, H., Day Jr., J.W., 2002. Landscape modeling of the Mississippi Delta. Bioscience 52, 357–365.

Mazzotti, S., Lambert, A., van der Kooij, M., Mainville, A., 2006. Coastal subsidence and relative sea-level rise in the Fraser River delta, Greater Vancouver, BC, from a combined CTM-InSAR, GPS, leveling, and tide gauge analysis. Eos Transaction AGU 87 (52) Fall Meet. Suppl., Abstract G23A-1263.

Mitsch, W.J., Gosselink, J.G., 2000. Wetlands, 3rd edition. John Wiley and Sons, New York. 920 pp.

Morris, J.T., Sundareshwar, P.V., Nietch, C.T., Kjerfve, B., Cahoon, D.R., 2002. Responses of coastal wetlands to rising sea level. Ecology 83, 2869–2877.

Mudd, S.M., Fagherazzi, S., Morris, J.T., Furbish, D.J., 2004. Flow, sedimentation, and biomass production on a vegetated salt marsh in South Carolina: toward a predictive model of marsh morphologic and ecologic evolution. In: Fagherazzi, S., Marani, M., Blum, L.K. (Eds.), The Ecogeomorphology of Tidal Marshes. American Geophysical Union Coastal and Estuarine Studies, Washington, D.C., pp. 165–187.

Murray, A.B., 2003. Contrasting the goals, strategies, and predictions associated with simplified numerical models and detailed simulations. In: Iverson, R.M., Wilcock, P.R. (Eds.), Prediction in Geomorphology. Geophysical Monograph, vol. 135. American Geophysical Union, Washington, D.C., pp. 151–165.

Patrick Jr., W.H., 1994. From wastelands to wetlands. Journal of Environmental Quality 23, 892–896.
Reed, D.J., 1995. The response of coastal marshes to sea-level rise: survival or submergence? Earth Surface Processes and Landforms 20, 39–48.
Reed, D.J., Cahoon, D.R., 1992. The relationship between marsh surface topography, hydroperiod, and growth of *Spartina alterniflora* in a deteriorating Louisiana salt marsh. Journal of Coastal Research 8, 77–87.
Reyes, E., White, M.L., Martin, J.F., Kemp, G.P., Day, J.W., Aravamuthan, V., 2000. Landscape modeling of coastal habitat change in the Mississippi Delta. Ecology 81, 2331–2349.
Shaw, A.L., Lintern, D.G., Hill, P.R., Houser, C., 2006. Factors controlling tidal flat response to sea level rise: Roberts Bank, British Columbia, Canada. Proceedings of the Coastal Dynamics 2005 International Conference, April 2005, Barcelona, Spain.
Smith, S.M., Warren, S., 2007. Determining ground surface topography in tidal marshes using watermarks. Journal of Coastal Research 23, 265–269.
Thursby, G.B., Chintala, M.M., Stetson, D., Wigand, C., Champlin, D.M., 2002. A rapid, nondestructive method for estimating aboveground biomass of salt marsh grasses. Wetlands 22, 626–630.
Turner, R.E., 1977. Intertidal vegetation and commercial yields of penaeid shrimp. American Fisheries Society Transactions 106, 411–416.
Vancouver Port Authority, 2005. Environmental Assessment Application for the Deltaport Third Berth Project: Roberts Bank, Delta, B.C. 868 pp.
van de Koppel, J., van der Wal, D., Bakker, J.P., Herman, P.M.J., 2005. Self- organization and vegetation collapse in salt marsh ecosystems. The American Naturalist 165, E1–E12.
Van der Wal, D., Pye, K., 2004. Patterns, rates, and possible causes of salt marsh erosion in the Greater Thames area (UK). Geomorphology 61, 373–391.
Vaughan, D.G., in press. West Antarctic Ice Sheet collapse — the fall and rise of a paradigm. Climatic Change.
Wells, J.T., Kemp, G.P., 1986. Interaction of surface waves and cohesive sediments: field observations and geologic significance. In: Mehta, A.J. (Ed.), Estuarine Cohesive Sediment Dynamics, Lecture Notes on Coastal and Estuarine Studies N°14. Springer, Berlin, Germany, pp. 43–65.
Williams, H.F.L., Hamilton, T.S., 1995. Sedimentary dynamics of an eroding tidal marsh derived from stratigraphic records of ^{137}Cs fallout, Fraser Delta, British Columbia, Canada. Journal of Coastal Research 11, 1145–1156.
Williams, H.F.L., Roberts, M.C., 1989. Holocene sea level change and delta growth: Fraser River Delta, British Columbia. Canadian Journal of Earth Sciences 26, 1657–1666.
Williams, K., Ewel, K.C., Stumpf, R.P., Putz, F.E., Workman, T.W., 1999. Sea level rise and coastal forest retreat on the west coast of Florida, USA. Ecology 80, 2045–2063.
Yang, S.L., Belkin, I.M., Belkina, A.I., Zhao, Q.Y., Zao, J., Zhu, J., Ding, P.X., 2003. Delta response to decline in sediment supply from the Yangtze River: evidence of the recent four decades and expectations for the next half century. Estuarine, Coastal and Shelf Science 57, 689–699.